Conference Proceedings of Science (CPS) January, 2026
ISSN: Volume: 1 Issue: 1
10

Article

Green synthesis of metal oxide nanoparticles and their dispersion on a polymer matrix and study their biological activity

Ali Ayoub Ibrahim[1*], Eman Jumaa Dheyab [2], Abdulqadier Hussien Al khazraji [1] Athraa mohamed Rashed[1]

[1]Department of Chemistry Science, College of Education for Pure Science, Diyala University, 32001 Diyala, Iraq.
[2]General Directorate of Education in Diyala, 32001 Diyala, Iraq.

ABSTRACT

Metallic nanoparticles (NPs) have enormous applications due to their remarkable physical and chemical properties. The synthesis of NPs has been a matter of concern because chemical methods are toxic. This study consists of two parts: The first part is the use of the leaves of the Iraqi lemon plant to prepare three metal oxides nanoparticles: copper oxide nanoparticles (CuO NPs), cobalt oxide nanoparticles (CoO NPs) and cadmium oxide nanoparticles (CdO NPs), which were analyzed using XRD, AFM, FESEM and FTIR spectroscopy. The second part is the dispersal of the nano-oxides prepared in the first part of the study on the surface of a polymer that was randomly selected for forming a binary compesite from a metal oxide nanoparticles / polymer. X-ray diffraction (XRD) analysis confirmed the pure single-phase cubic structure of green synthesized CdO NPs, the size of nanoparticles was 102 nm. The biological activity of metal oxides nanoparticles has excellent for B1, in concentration 25 µg/mL gave a higher diameter than the concentration of 50 µg/mL. While the compound B5, it gave an identical effect diameter for both concentrations used, amounting to (40 mm). We also note that the compound B6, at a concentration of 25 µg/mL, gave a larger diameter of (60 mm) compared to the concentration of 50 µg/mL. In contrast, the compound B7, at a concentration of 25 µg/mL, gave a smaller area compared to the concentration of 50 µg/mL. Moreover, during the green synthesis, unreacted metals are drained, which causes contamination to the ecosystem.

Keywords Eco-Friendly method, Metallic nano-oxides, Polymer, E. coli bacterial, S. aureus bacterial.

***Corresponding Author**

Ali Ayoub Ibrahim
Department of Chemistry Science, College of Education for Pure Science, University of Diyala, Baqubah City, Diyala Governorate,3200, Iraq.
Email: ali.ayoub.ibraheem@uodiyala.edu.iq

1. INTRODUCTION

Metal oxides hold an important position in nanoscale applications, due to their good semiconductors. They are therefore widely used in the construction of sensors, fuel cells, electronic circuits, electromagnetic devices, anti-corrosion coatings, as well as catalysts, medical uses, and antibacterial properties [1, 2]. Although many chemical methods are available for preparing metal nanoparticles, they are toxic and hazardous. Increasing environmental concerns regarding chemical preparation have led to attempts to find bio-based alternatives. One such method is preparation using plant extracts. In recent years, researchers have become increasingly interested in preparing and studying nanoscale metal oxides due to their growing applications. It has been found that the various properties of these oxides change significantly at the nanoscale compared to the conventional scale, which results in a complete change in properties[3]. In 2014, Suresh and his group prepared magnesium oxide (MgO) [4], using Nephelium lappaceum L. peels. This method was effectively used to synthesize magnesium oxide. XRD and SEM revealed the morphology of the biosynthesized nanoparticles, showing crystallization and spherical particles formed with the size of magnesium oxide nanoparticles at 60-70 In 2015,

Sarganan and his team prepared a ZnO/Ag/CdQ ternary nanocomposite using a thermal decomposition method. The resulting nanocomposite was characterized using FESEM, XRD, UV-Vis, TEM, and XPS spectroscopy. The secondary ZnO/Ag/CdQ ternary composite was optimized for photocatalytic activity using visible light irradiation to degrade methylene blue and methyl orange dyes compared to the binary ZnO/Ag and ZnO/CdQ ternary nanocomposites. The secondary ZnO/Ag/CdQ composite was also used in the decomposition of industrial wastewater. A real sample analysis revealed that it degraded over 90% in 210 minutes under visible light irradiation. The small size, high surface area, and synergistic effect of ZnO/Ag/CdQ are responsible for the high photocatalytic activity. These results also demonstrated that Ag nanoparticles induced visible light activity and facilitated efficient charge separation in the Ag/ZnO/dO secondary complex, thus improving the photocatalytic performance [5, 6]. Magnesium oxide nanoparticles were prepared in 2017 using a green synthesis method, using various plant extracts, including orange, lemon, vinegar, and tamarind. This preparation method is environmentally friendly, meaning it is green and relies on plant materials with non-toxic and inexpensive chemicals[7]. The variety of engineered nanomaterials is designed with different sizes and shapes to have the properties which are not present in bulk samples of the same materials [8]. CoO and Co_3O_4 more stable from other cobalt oxides, as well as they have high stability of kinetically at room temperature, hence required a lot of attention in the scientific researches due to their promise applications [9].

2. METHOD

2-1- Preparation of the Lemon Leaf Extract

The green reducing and stabilizing agent was prepared from the *Lemon* leaves collected from the Diyala governorate gardens in Iraq. The leaves were washed using deionized water to remove impurities and cut them into small pieces. 25 g of cut leaves were put in 100 mL deionized water and set the temperature at 80°C. After some time, the water turned greenish, indicating leaf extract formation in the water. The filtered extract was poured into the burette; this extract would be used as a reducing agent for nanoparticle synthesis [10], Figure (1).

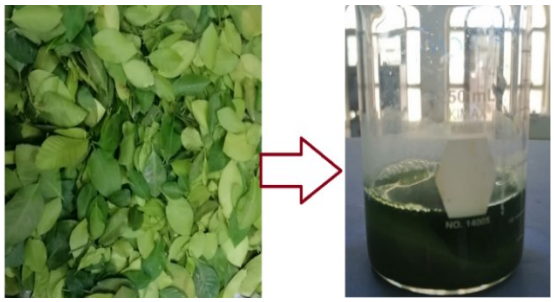

Figure 1. Weibull distribution of all filler concentrations

2-2 Synthesis of metal oxides nanoparticles

(CuCl2.6H2O, CoCl2.6H2O and CdCl2) were used as the precursors. For the synthesis, 25 ml of moringa extract was added from the burette, to different doses of the precursors which ranged from 1 g, then it was transferred into ceramic crucibles and heated at 80 ◦C under a vigorous magnetic stirrer and sodium hydroxide (0.1 M NaOH) solution was introduced slowly to the solution under a stirrer until the pH=12. After 2 hours, the obtained precipitates were filtered using a Buckner funnel, washed with distilled water several times, and dried in an oven for 2 hours. calcination was carried out in the furnace at 550 ºC for 3 hours to remove any contamination . As shown in Figure (2).

Figure 2. Synthesis of CdO- CuO- CoO NPs using metal chlorid salts as sources of metal by *lemon* leaves extract

2-3 Synthesis of compesite (MO)/ Polymer

Metal oxide nanoparticles/ polymer was prepared from dissolve 0.3g from oxide nanoparticles in 20ml ethanol with stirrer for 45min. in another bucker we were dissolve about 0.3g from the tetra-hydrofuran (THF) for 30min after that add all the oxide nanoparticles mixture with slowly stirrer under 70 C^0 for 30min. transfer the mixture to the oven under 70 C0 to evaporation alcohol and to dry the material to get MONPs/ Polymer that is shown in fig (3).

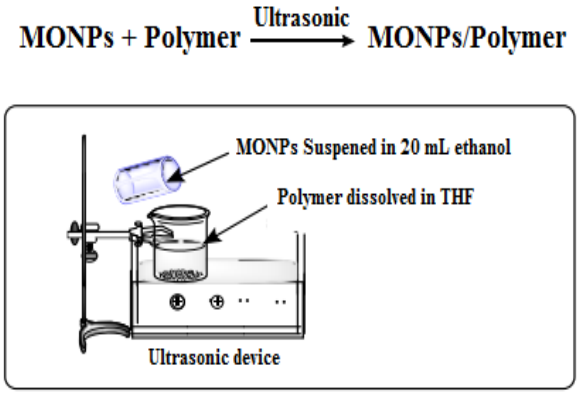

Figure 3. Preparation the compesite (MO)/ Polymer.

Table 1. The performance of ...

Variable	Speed (rpm)	Power (kW)
X	10	8.6
Y	15	12.4
Z	20	15.3

3. RESULTS AND DISCUSSION

3.1 Infrared Spectroscopy (FTIR) of metal hydroxides and oxides nanoparticles.

FTIR spectra of samples prepared from nanoparticles of metal hydroxides and oxides (copper, cobalt, and cadmium) are shown. The FTIR spectrum of the copper hydroxide sample in Figure 4 shows a strong peak at 3417 cm I | Corresponding to the free OH group and the peak at 1-356 results from the OH group bonded to hydrogen and the appearance of a peak at 1604 cm is due to the bending of the hydroxyl group bonded to hydrogen (1999 Frost R L and Kloprogge J). The spectrum also shows peaks at 1388 cm and 1288 cm, which indicate the Cu-OH bond and an absorption peak at 1064 cm, which indicates the vibrations of (Cu-OH), in addition to two absorption peaks at 478 cm and 17 due to the vibrational mode of the (0) bond 17 [11] . Compared to Figure 4, the spectrum (in red) shows the FTIR spectrum of secondary copper oxide particles CuO-NPs in the range of 3900-450 at room temperature, where it showed several peaks with the disappearance of the trend peaks of the hydroxide group. In contrast, the characteristic section for copper oxide is located between 1439,501 and 817 cm, which indicates the formation of The nanostructure of CuO and the weak section stretching frequency of the Cu-Cu bond observed between 3525 cm-3379 cm- correspond to the FTIR spectral results confirm the presence of phytochemicals in the plant extract used.[12]

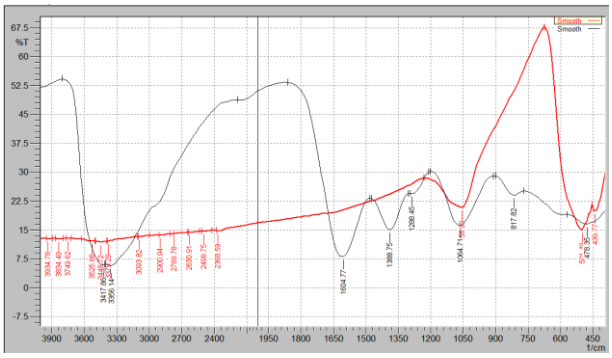

Figure 4. FTIR spectra of $Cu(OH)_2$ nanoparticles (black) and CuO nanoparticles (red)

For cadmium hydroxide ($Cd(OH)_2$) synthesized using lemon leaf extract, the FTIR spectrum (black curve, Figure 5) displays a broad O–H stretching band at 3417 cm^{-1}, which becomes significantly weaker in the CdO spectrum (red curve).The FTIR results also show several vibrational peaks at 617, 1059, 1419, 1573, and 2947 cm^{-1}, indicating the presence of organic phytochemicals from the plant extract that contributed to reduction and stabilization processes[12] .

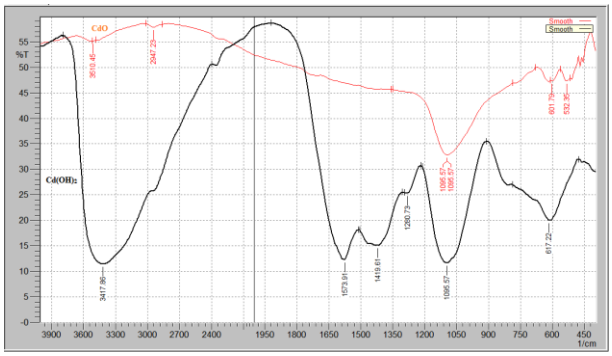

Figure5. FTIR spectra of $Cd(OH)_2$ nanoparticles (black) and CdO nanoparticles (red).

For cobalt hydroxide ($Co(OH)_2$) and cobalt oxide (CoO) nanoparticles, FTIR analysis was performed to identify the functional groups involved in reduction and stabilization. The spectrum (black curve, Figure 6) of $Co(OH)_2$ exhibits an O–H stretching band at 3417 cm^{-1}, which becomes weaker and slightly shifts to 3464 cm^{-1} after calcination, due to the presence of polyphenolic compounds from the lemon extract. Characteristic peaks between 1126–1634 cm^{-1} correspond to aromatic ring vibrations and bending modes of O–H and C–O in alcohols and carboxylic acids, indicating that these biomolecules play a key role in forming and capping the CoO nanoparticles.

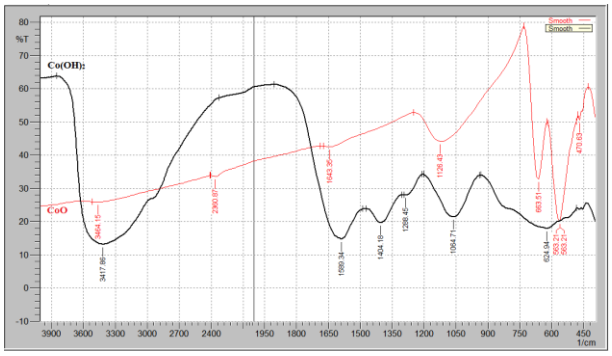

Figure 6. FTIR spectra of $Co(OH)_2$ nanoparticles (black) and CoO nanoparticles (red).

3.2. X-Ray Diffraction (XRD) Analysis

The XRD technique was employed to analyze the crystalline phases of the synthesized metal oxide nanoparticles and their corresponding polymer nanocomposites, as shown in Figures 7. For CuO nanoparticles (Figure 8), the diffraction pattern revealed distinct peaks at $2\theta = 35.9°$ and 39.3°, which correspond to the characteristic planes of monoclinic CuO and are in strong agreement with reported literature values [11]. When CuO nanoparticles were dispersed in the polymer matrix (Figure 9), noticeable shifts and broadening of diffraction peaks were observed, along with the appearance of new peaks and reduced peak intensities. These changes indicate successful dispersion and interaction between CuO nanoparticles and the polymer matrix.

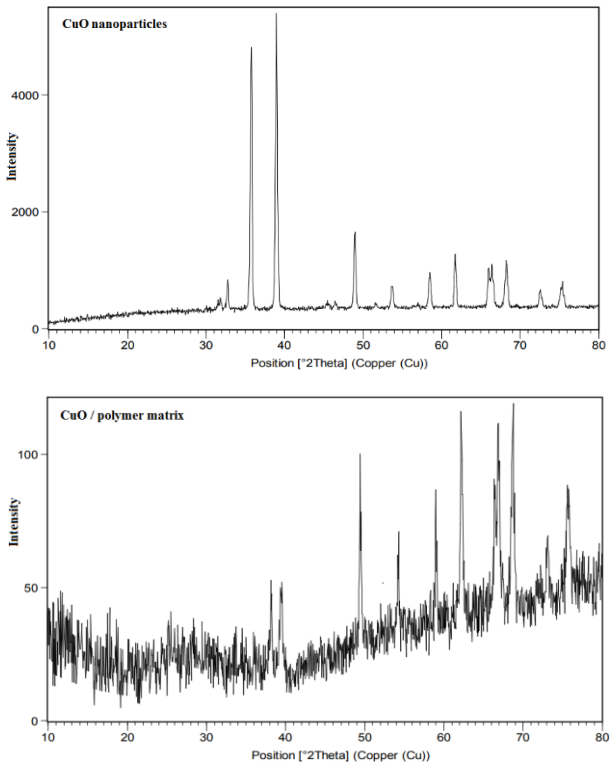

Figure 4 . XRD pattern of CuO NPs (A) and (B) CuO/ Polymer matrix .

For CoO nanoparticles (Figures 8a.b), the diffraction peaks observed at 2θ = 18.95°, 31.22°, 36.80°, and 44.77° correspond to the cubic CoO phase, consistent with previous studies [10]. After composite formation (CoO/polymer), the peak intensities decreased, with slight broadening, but the overall crystal structure remained intact. This suggests that the polymer had minimal impact on the crystallinity of CoO, likely due to the high purity and uniformity of the CoO nanoparticles compared to CuO.

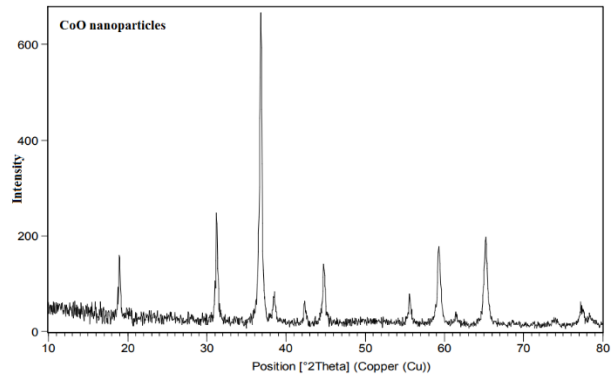

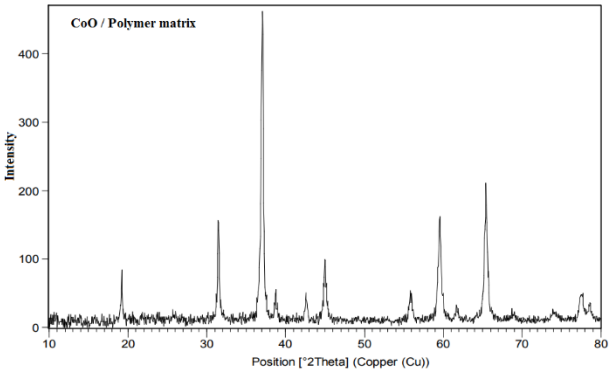

Figure 8 . XRD pattern of CoO NPs (A), and (B) CoO/Polymer.

XRD patterns of CdO NPs showed absorbance of the diffraction peaks at 2θ values. The estimated particle size using the relative intensity peak for CdO-NPs (chemically synthesized CdO NPs) was 102.8694 nm, and sharp peaks indicate that particles were crystalline in nature. The peaks at the diffraction angles of 33.325, 55.658, and 66.169° are indexed to the (111), (220) and (311) planes, respectively (Figure 9). [13]

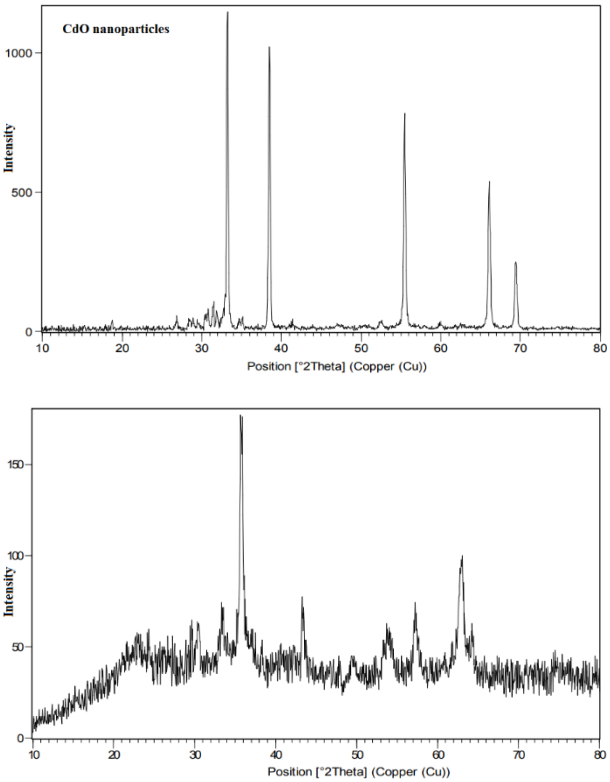

Figure 9. XRD pattern of CdO NPs (A), and (B) CdO/Polymer.

The average crystallite sizes (D) were calculated using the Debye–Scherrer equation, and the results are summarized below:

Sample	D, nm
CuO	10.63689
CoO	76.20868
CdO	102.8694
CuO/ Polymer	365.4899
CoO / Polymer	349.493
CdO / Polymer	106.1786

These results indicate that the particle size follows the order: CdO > CoO > CuO, and that particle sizes increased slightly upon polymer incorporation. This is attributed to the influence of the polymer matrix on nanoparticle dispersion, which can either reduce or enhance peak sharpness depending on the level of aggregation.

3.3. Atomic Force Microscopy (AFM)

Atomic Force Microscopic allows us resultant microscopic notion on to plot topographies representing the surface alleviation and the structure of surface. This technique refers to digital images that allow quantitative measurements of surface features, such as root mean square roughness, (Rq) or average roughness (Ra) and the analysis of images from different perspectives including 3D simulation (22). Fig. 10 a and b displayed spherical clusters with an average size of 12.38 nm, showing a high degree of agglomeration.[14]

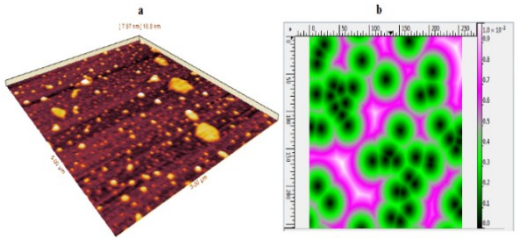

Figure10: Atomic force microscope (AFM) a-three dimension image of (CuO) NPS, b- two dimension of CuO.

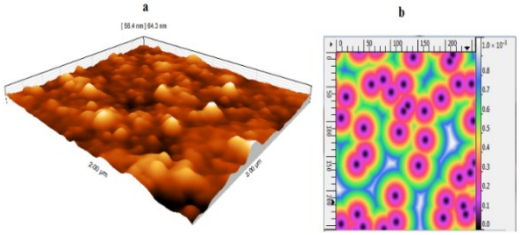

Figure11: Atomic force microscope (AFM) a- three dimension image of (CuO NPS /Polymer), b- two dimension of CuO NPS /Polymer.

When incorporated into the polymer (Figure 11a, b), the CuO/polymer nanocomposite exhibited a more uniform dispersion with reduced aggregation and a larger average particle size of 60 nm, indicating that the polymer matrix facilitated nanoparticle stabilization and distribution. Similarly, the CoO nanoparticles (Figure 12a,b) showed compact clusters with an average particle size of 12.25 nm, while in the CoO/polymer composite (Figure 13a,b), the particles were well dispersed with an increased average size of 105.8 nm.

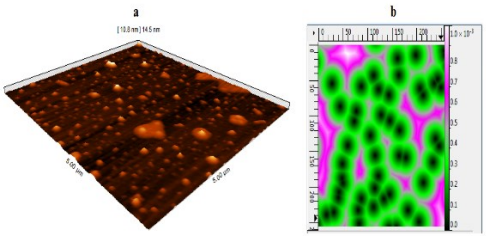

Figure12: Atomic force microscope (AFM) a-three dimension image of (CoO NPS), b- two dimension of CdO NPS.

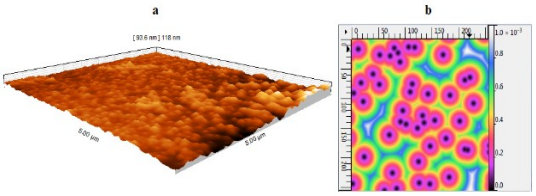

Figure13: Atomic force microscope (AFM) a- three dimension image of (CoO NPS /Polymer), b- two dimension of CoO NPS /Polymer.

For CdO nanoparticles (Figure 14a,b), AFM analysis revealed an average particle size of 18.25 nm, which increased to 104.7 nm in the CdO/polymer composite. In all composites, the polymer matrix was found to significantly influence both particle size and aggregation behavior, confirming effective nanoparticle dispersion.

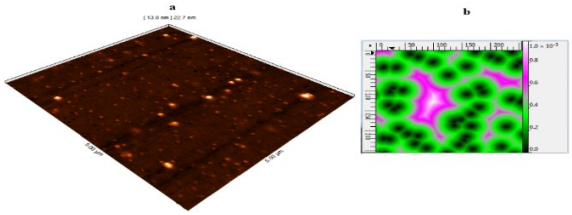

Figure12: Atomic force microscope (AFM) three dimension image of (CdO NPS, b- two dimension of CdO NPS.

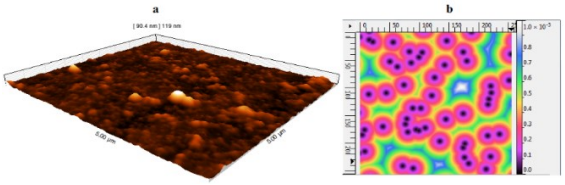

Figure13:Atomic force microscope (AFM) three dimension image of (CdO NPS /Polymer), b- two dimension of CdO NPS /Polymer.

The biological activity of metal oxides nanoparticles

Evaluation of antibacterial activity was carried out for synthesized CuO,CuO/polymer, CoO,CoO/polymer, CdO, CdO/polymer NPs using *lemon* leaf extract against two gram positive and two gram negative bacterial *(E. coli and S. aureus).*

As shown in Table (2) we used two different concentrations,(25 µg/mL) and (50 µg/mL), it is worth

noting that these isolates were chosen for their importance in the medical field, as they cause many diseases and have a high capacity to resist chemical therapeutic materials and antibiotics.

Table 2: Shows the symbols of the prepared compounds.

Symbol	Sample
B1	Polymer
B2	CuO NPs/ Polymer
B3	CoO NPs/ Polymer
B4	CdO NPs/ Polymer
B5	CuO NPs
B6	CdO NPs
B7	CoO NPs

❖ *E. coli* bacterial:

Figural .17 shows the various zones of inhibition (mm), when the panel of bacteria was treated with (25 µg/mL) and (50 µg/mL) of CuO,CuO/polymer, CoO,CoO/polymer, CdO, CdO/polymer samples. B1 has excellent antibacterial activity the concentration of 25 µg/mL gave a higher diameter than the concentration of 50 µg/mL, as shown in Table (3). While the compound B5, it gave an identical effect diameter for both concentrations used, amounting to (40 mm). We also note that the compound B6, at a concentration of 25 µg/mL, gave a larger diameter of (60 mm) compared to the concentration of 50 µg/mL. In contrast, the compound B7, at a concentration of 25 µg/mL, gave a smaller area compared to the concentration of 50 µg/mL, as shown in Table (3).

❖ *S. aureus* bacterial:

The prepared compound (B1) represented by the polymer gave high inhibitory activity towards S. aureus bacteria at the two concentrations used in this study, as B1 gave at the concentration of 25 µg/ml a high inhibition diameter (50 mm) compared to the concentration of (50 µg/ml) which had an effective area of (40 mm), as shown in Table (3).

Also, the nano oxides ((B5 prepared at a concentration of 25 µg/ml)) which represents CuO NPs gave a high inhibition area estimated at greater than (>50 mm) compared to a concentration of 50 µg/ml)), while in the case of the compound (B6) which represents CdO NPs, it gave at both concentrations almost equal effect area (50 mm and 48 mm). The compound CoO NPs gave an inhibition area estimated at >50 mm)) at the two different study concentrations, as shown in Table (3) as well.

The biological activity of binary their composite

❖ *E. coli* bacterial:

The CuO NPs/Polymer complex at a concentration of 25 gave a lower inhibitory effect area than the concentration of 50 µg/ml, and the same applies to the CoO NPs/Polymer complex at a concentration of 25 µg/ml, which also gave a lower inhibitory effect area than the concentration of 50 µg/ml. As for the complex (B4) at a concentration of 25 µg/ml, which represents CdO NPs/Polymer, it gave a lower inhibitory effect area at the concentration of 50 µg/ml; as shown in Table No. (3)

❖ *S. aureus* bacterial:

Through the results shown in Table (3), we note that all oxides and their binary complexes (B2-B7) at the two selected study concentrations of 25µg/ml and 50µg/ml gave a high inhibitory effect area of (>50mm), which is evidence of their very high effectiveness.

Table 3: Shows the types of bacteria used in the study at two different concentrations (25µg/mL) and (50µg/mL).

Sample	Concentration (µg / ml)	Zone of inhibition (in mm) Bacteria	
		E. coli	*S. aureus*
B1	25	31	40
	50	37	50
B2	25	37	52
	50	40	44
B3	25	43	34
	50	45	50
B4	25	36	52
	50	37	50
B5	25	40	42
	50	40	50
B6	25	42	52
	50	60	48
B7	25	31	52
	50	57	52
Chloramphenicol	25	24	15
	50	21	24
Gentamycin	25	28	24
	50	21	25
Imipenem	25	24	26
	50	26	22
Ciprofloxacin	25	0	0
	50	24	28
Levofloxacin	25	21	32
	50	28	28
Clindamycin	25	28	24
	50	21	26
DMSO	25	0	0
	50	0	0

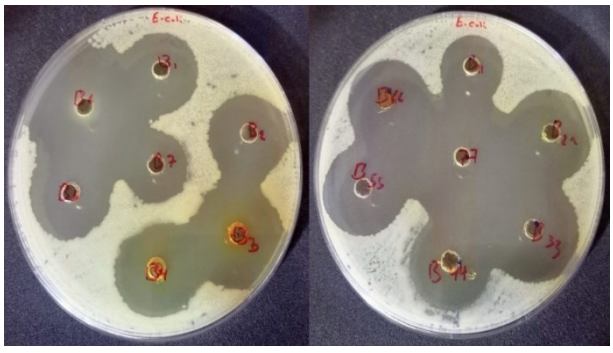

Figure 17: Shows a comparison of *E. coli bacteria* in the presence of the two selected study concentrations (25 µg/mL) and (50 µg/mL).

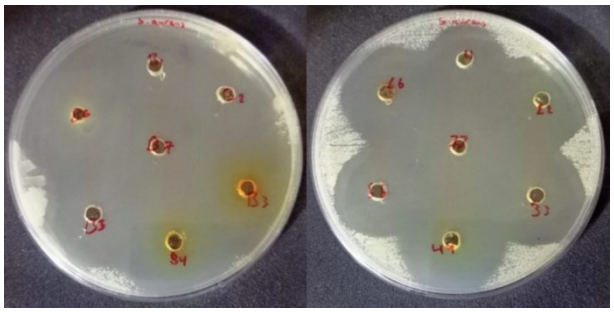

Figure 18: Shows a comparison of *S. aureus bacterial* bacteria in the presence of the two selected study concentrations (25 µg/mL) and (50 µg/mL).

4. CONCLUSION

Green synthesis method was successfully used for CuO,CoO,CdO nanoparticle production, and by impregnation method, the CuO/polymer, CoO/polymer and CdO/polymer were successfully synthesized. XRD revealed CuO,CoO,CdO nanoparticle synthesis with average particle size and the lattice parameter CdO > CoO > CuO are 102.8694, 76.20868 and 10.63689 , and that particle sizes increased slightly upon polymer incorporation. This is attributed to the influence of the polymer matrix on nanoparticle dispersion, which can either reduce or enhance peak sharpness depending on the level of aggregation. The AFM image of the nano oxide was almost irregular in shape and conglomerates some structures like islands were obtained with an average size diameter of 12-18 nm for all the nano oxide that were prepared. Furthermore, there was a minor variation in response to biological activities study. Based on the results, it can be concluded that although green-synthesized NPs might be less compatible to the living system, there is variation in the characteristics of nanoparticles. The green synthesis approach also produces more waste (unreacted metal) that is drained into the water f low. This causes contamination in water, soil, and, of course, the food chain, thereby causing a serious threat to humans.

ACKNOWLEDGEMENTS

Our thanks and appreciation to the staff of the laboratories of the Department of Chemistry and Biological Sciences at the College of Education for Pure Sciences

REFERENCES

[1] R. S. Patil, et al., "Synthesis and enhancement of photocatalytic activities of ZnO by silver nanoparticles," Spectrochimica Acta Part A: Molecular and Biomolecular Spectroscopy, vol. 122, pp. 113-117, 2014.

[2] M. S. Chavali and M. P. Nikolova, "Metal oxide nanoparticles and their applications in nanotechnology," SN applied sciences, vol. 1, p. 607, 2019.

[3] M. Shah and T. Ahmad, Principles of nanoscience and nanotechnology: Alpha Science International, 2010.

[4] S. Suresh, "Investigations on synthesis, structural and electrical properties of MgO nanoparticles by sol–gel method," J Ovonic Res, vol. 10, pp. 205-210, 2014.

[5] R. Saravanan, et al., "ZnO/Ag/CdO nanocomposite for visible light-induced photocatalytic degradation of industrial textile effluents," Journal of colloid and interface science, vol. 452, pp. 126-133, 2015.

[6] S. Balachandran, et al., "Facile fabrication of highly efficient, reusable heterostructured Ag–ZnO–CdO and its twin applications of dye degradation under natural sunlight and self-cleaning," RSC advances, vol. 4, pp. 4353-4362, 2014.

[7] R. Prasanth, et al., "Green synthesis of magnesium oxide nanoparticles and their antibacterial activity," Indian Journal of Geo Marine Sciences, vol. 48, pp. 1210-1215, 2019.

[8] A. Barhoum, et al., "Review on natural, incidental, bioinspired, and engineered nanomaterials: history, definitions, classifications, synthesis, properties, market, toxicities, risks, and regulations," Nanomaterials, vol. 12, p. 177, 2022.

[9] M. F. Gazulla, et al., "Characterization of cobalt oxides transformations with temperature at different atmospheres," Int J Chem Sci Res, vol. 17, p. 312, 2019.

[10] A. M. Rashed and A. H. Al Khazraji, "Synthesis of Carbon Nanotubes Using Plant Source and Study their Properties," NeuroQuantology, vol. 19, pp. 95-102, 2021.

[11] [M. I. Nabila and K. Kannabiran, "Biosynthesis, characterization and antibacterial activity of copper oxide nanoparticles (CuO NPs) from actinomycetes," Biocatalysis and agricultural biotechnology, vol. 15, pp. 56-62, 2018.

[12] A. El-Trass, et al., "CuO nanoparticles: synthesis, characterization, optical properties and interaction with amino acids," Applied Surface Science, vol. 258, pp. 2997-3001, 2012.

[13] H. Nagabhushana, et al., "Facile EGCG assisted green synthesis of raspberry shaped CdO nanoparticles," Journal of Alloys and Compounds, vol. 669, pp. 232-239, 2016.

[14] Z. J. Shanan, et al., "Structural analysis of chemical and green synthesis of CuO nanoparticles and their effect on biofilm formation," Baghdad Science Journal, vol. 15, p. 14, 2018.